Journal of Virology

Progression From IgD$^+$ IgM$^+$ to Isotype-Switched B Cells Is Site Specific during Coronavirus-Induced Encephalomyelitis

Timothy W. Phares, Krista D. DiSano, Stephen A. Stohlman and Cornelia C. Bergmann

J. Virol. **2014, 88(16):8853. DOI: 10.1128/JVI.00861-14.**
Published Ahead of Print 28 May 2014.

JVI Journals.ASM.org

Progression From IgD$^+$ IgM$^+$ to Isotype-Switched B Cells Is Site Specific during Coronavirus-Induced Encephalomyelitis

Timothy W. Phares,[a] Krista D. DiSano,[a,b] Stephen A. Stohlman,[a] Cornelia C. Bergmann[a]

Department of Neurosciences, Lerner Research Institute, Cleveland Clinic Foundation, Cleveland, Ohio, USA[a]; School of Biomedical Sciences, Kent State University, Kent, Ohio, USA[b]

ABSTRACT

Various infections in the central nervous system (CNS) trigger B cell accumulation; however, the relative dynamics between viral replication and alterations in distinct B cell subsets are largely unknown. Using a glia-tropic coronavirus infection, which is initiated in the brain but rapidly spreads to and predominantly persists in the spinal cord, this study characterizes longitudinal changes in B cell subsets at both infected anatomical sites. The phase of T cell-dependent, antibody-independent control of infectious virus was associated with a similar recruitment of naive/early-activated IgD$^+$ IgM$^+$ B cells into both the brain and spinal cord. This population was progressively replaced by CD138$^-$ IgD$^-$ IgM$^+$ B cells, isotype-switched CD138$^-$ IgD$^-$ IgM$^-$ memory B cells (B_{mem}), and CD138$^+$ antibody-secreting cells (ASC). A more rapid transition to B_{mem} and ASC in spinal cord than in brain was associated with higher levels of persisting viral RNA and transcripts encoding factors promoting B cell migration, differentiation, and survival. The results demonstrate that naive/early-activated B cells are recruited early during coronavirus CNS infection but are subsequently replaced by more differentiated B cells. Furthermore, viral persistence, even at low levels, is a driving force for accumulation of isotype-switched B_{mem} and ASC.

IMPORTANCE

Acute and chronic human CNS infections are associated with an accumulation of heterogeneous B cell subsets; however, their influence on viral load and disease is unclear. Using a glia-tropic coronavirus model, we demonstrate that the accumulation of B cells ranging from early-activated to isotype-switched differentiation stages is both temporally and spatially orchestrated. Acutely infected brains and spinal cords indiscriminately recruit a homogeneous population of early-activated B cells, which is progressively replaced by diverse, more differentiated subsets. The latter process is accelerated by elevated proinflammatory responses associated with viral persistence. The results imply that early-recruited B cells do not have antiviral function but may contribute to the inflammatory environment or act as antigen-presenting cells. Moreover, CNS viral persistence is a driving force promoting differentiated B cells with protective potential.

Central nervous system (CNS) inflammation during microbial infections, autoimmunity, or spinal cord injury is associated with recruitment of various B cell subsets, including antibody-secreting cells (ASC) (1–5). In cases of acute encephalitis, B cell and antibody (Ab) accumulation is transient; however, humoral responses persist during chronic CNS diseases such as subacute sclerosing panencephalitis and multiple sclerosis (MS) (6–8). However, the mechanisms driving the accumulation of various B cells as well as their phenotype, role, and precursor relationships to ASC are poorly defined. In patients with subacute sclerosing panencephalitis, the majority of oligoclonal Ab bands are measles virus specific, suggesting that persisting viral antigen drives local humoral responses (6, 9), yet their role is difficult to assess. A large proportion of CNS-localized ASC in Sindbis virus and neurotropic coronavirus infection models is also virus specific and correlated with protection (2, 4, 10).

One mechanism thought to promote local CNS B cell differentiation and Ab production involves the formation of ectopic follicle-like structures, as described previously for neuroborreliosis and MS (11–13). Ectopic follicle formation in the CNS during microbial or autoimmune inflammation is supported by the constitutive and induced expression of several factors regulating B cell responses in lymphoid organs. Among these factors are the chemokines CXCL13, CCL19, and CCL21, which guide B cell migration within lymph nodes, as well as CXCL9, CXCL10, and CXCL12, which are implicated in ASC trafficking (3, 14–16). Moreover, factors involved in both B cell differentiation, such as interleukin-6 (IL-6), IL-10, and IL-21, as well as B cell survival, namely, B cell-activating factor of the tumor necrosis factor (TNF) family (BAFF) and a proliferation-inducing ligand (APRIL), are also upregulated during virus- or autoantigen-induced CNS inflammation (3, 15, 17–19). Although CXCL13 is implicated in the formation of ectopic follicle-like structures in the CNS (11–13, 16), there is no evidence for ectopic lymphoid follicles during Sindbis virus infection, despite the expression of CXCL13 and CCL19 and the presence of various B cell subsets within the CNS (2, 15). Increasing proportions of isotype-switched memory B cells (B_{mem}) and ASC during Sindbis virus CNS persistence thus suggested that B cell subset alterations toward a more differentiated phenotype may reflect their egress into circulation from peripheral maturation sites and survival in the CNS (2). Early B cell

Received 25 March 2014 **Accepted** 21 May 2014
Published ahead of print 28 May 2014
Editor: S. Perlman
Address correspondence to Cornelia C. Bergmann, bergmac@ccf.org.

doi:10.1128/JVI.00861-14

accumulation with an increasing proportion of ASC during viral persistence is also evident during glia-tropic coronavirus infection (3, 4, 20). Moreover, in this model, direct ASC recruitment from the periphery was implicated by CXCR3-dependent ASC accumulation within the CNS, subsequent to peak peripheral expansion (20). The gradual downregulation of major histocompatibility complex (MHC) class II on ASC further suggested ongoing local CNS differentiation of plasmablasts or preferential survival of more differentiated ASC (10).

Infection with the glia-tropic coronavirus strain JHMV was thus used to elucidate how a differential viral load and/or the inflammatory milieu affects the progression of humoral responses at distinct sites within the CNS. JHMV replication is initiated in the brain, but the virus rapidly spreads to and predominantly persists in the spinal cord (21–23). T cells control infectious virus in the CNS within 2 weeks independent of humoral immunity; however, persisting viral RNA is controlled by ASC (24, 25). While B cells are recruited during acute infection, ASC do not emerge in the CNS until day 14 postinfection (p.i.), increase in numbers significantly by day 21, and remain at declining numbers through persistence (3, 23). An essential role of sustained CNS Ab production in ongoing protection (24, 25) was confirmed in infected CXCR3-deficient mice, which exhibit impaired humoral responses in the CNS but not the periphery (20).

The data reported here demonstrate that B cells recruited to the CNS early during acute inflammation display a naive/early-activated IgD^+ IgM^+ phenotype. A gradual loss of IgD expression and increased numbers of $CD138^+$ ASC and IgD^- $CD138^-$ B_{mem} indicated replacement by more differentiated B cells as infection progressed into persistence. This transition was more rapid and robust in the spinal cord than in the brain, despite similar numbers of early-recruited B cells. These studies suggest that naive/early-activated B cells migrate indiscriminately to sites of acute inflammation as bystanders but are replaced by more differentiated B cells derived from peripheral germinal centers. During this transition, site-specific accumulation and survival of B_{mem} and ASC within the CNS are clearly dictated by the magnitude of viral persistence, which in turn drives ongoing inflammatory responses, including factors promoting migration and survival of differentiated isotype-switched B cells.

MATERIALS AND METHODS

Mice, virus infection, and virus titers. C57BL/6 mice were purchased from the National Cancer Institute (Frederick, MD). All mice were housed under pathogen-free conditions at an accredited facility at the Cleveland Clinic Lerner Research Institute. Mice were infected at 6 to 7 weeks of age by intracranial injection into the left cerebral hemisphere with 1,000 PFU of the J.2.2v-1 monoclonal Ab (MAb)-derived glia-tropic JHMV variant in 30 μl sterile phosphate-buffered saline (PBS) (23, 26). Notably, intracranial injection of sterile PBS alone does not elicit an increase in the number of infiltrating $CD45^{hi}$ cells by flow cytometry 5 days later compared to naive mice. All animal experiments were performed in accordance with guidelines approved by the Cleveland Clinic Lerner Research Institute Institutional Animal Care and Use Committee. Virus titers within the brain and spinal cord were determined in clarified supernatants by a plaque assay using the murine delayed brain tumor astrocytoma (DBT) cell line, as described previously (26). Plaques were counted after 48 h of incubation at 37°C, and titers were calculated per mg tissue. Typical weights of brain and spinal cord were 397 ± 10 mg and 80 ± 2 mg, respectively.

CNS Ab. Virus-specific immunoglobulin within the CNS was detected in clarified spinal cord or brain supernatants by an enzyme-linked immunosorbent assay (ELISA), as described previously (20). Briefly, 96-well plates were coated with 100 μl of a serum-free supernatant derived from JMHV-infected DBT cells and incubated overnight at 4°C. Plates were washed with PBS-Tween 20, and nonspecific binding was blocked with 10% fetal calf serum in PBS overnight at 4°C. Samples were added and incubated overnight at 4°C. After washes, bound IgM and IgG2a were detected by using biotinylated goat anti-mouse IgM (Jackson ImmunoResearch, West Grove, PA) or goat anti-mouse IgG2a (Southern Biotech, Birmingham, AL). Secondary Ab was detected by using streptavidin horseradish peroxidase (BD Bioscience) followed by 3,3′,5,5′-tetramethylbenzidine (TMB reagent set; BD Bioscience). Optical densities were read at 450 nm on a SpectraMax Mz microplate reader (Molecular Devices, Sunnyvale, CA). Data are expressed as arbitrary units/mg tissue, where 1 arbitrary unit equals an absorbance of 0.1. Levels were calculated by using the following formula: (absorbance) × dilution factor × volume of clarified brain or spinal cord homogenate. Background levels from naive mice were subtracted.

Blood-brain barrier permeability. Blood-brain barrier (BBB) permeability was assessed by using sodium fluorescein (NaF) to detect fluid-phase shifts between the circulation and CNS, as described previously (27). Briefly, mice received 100 μl of 10% NaF in PBS intraperitoneally, and cardiac blood was collected 10 min later. Mice were transcardially perfused with 10 ml of PBS, and spinal cord and brain were removed. Tissues were homogenized in PBS, and NaF content in clarified supernatants was measured on a SpectraMax Mz microplate reader by using standards ranging from 125 to 4,000 μg. The NaF content in the CNS supernatant was normalized to serum NaF content by using the following formula: (mg fluorescent brain tissue/mg of protein)/(mg fluorescent sera/μl of blood). Data are expressed as fold increases in fluorescence in the brain or spinal cord, with the levels from uninfected mice being set at a value of 1.

Flow cytometry and fluorescence-activated cell sorting (FACS). Brains and spinal cords from groups of 6 to 8 mice perfused with PBS were homogenized in ice-cold Tenbroeck grinders in Dulbecco's PBS. Mononuclear cells were recovered from the 30%–70% interface of a Percoll step gradient (Pharmacia, Piscataway, NJ) following centrifugation at 850 × *g* for 30 min at 4°C, as detailed previously (28). Single-cell suspensions from cervical lymph nodes (CLN) were prepared as described previously (28). Phenotypic analysis of pooled cells was performed by staining with MAbs specific for CD19 (MAb 1D3), CD45 (30-F11), CD138 (281-2), IgD (11-26), IgG2a/b (R2-40) (all from BD Bioscience), and IgM (eB121-15F9) (eBioscience). For surface and intracellular detection of IgG2a/b, cells were stained with biotin-labeled anti-IgG2a/b Ab and allophycocyanin-conjugated streptavidin. Cells were then permeabilized with Cytofix/Cytoperm reagent (BD Bioscience), stained with fluorescein isothiocyanate-labeled anti-IgG2a/b Ab, and analyzed on a BD FACSAria instrument (BD, Mountain View, CA) using FlowJo 10 software (Tree Star, Ashland, OR).

For RNA expression in CNS-derived B cell subsets, pooled spinal cords ($n = 6$ to 8) were digested with collagenase and purified by using a BD FACSAria instrument. In brief, spinal cords were finely minced with a razor blade and digested in 5 ml of RPMI supplemented with 10% fetal calf serum, 250 μl of collagenase D (100 mg/ml) (Roche Diagnostics, Indianapolis, IN), and 50 μl of DNase I (1 mg/ml) (Roche Diagnostics) for 40 min at 37°C. Collagenase and DNase I activities were terminated by the addition of 500 μl of 0.1 M EDTA (pH 7.2) at 37°C for 5 min. Following centrifugation, cells were washed with RPMI supplemented with 25 mM HEPES, and mononuclear cells were recovered from the 30%–70% interface of a Percoll gradient as described above. $CD19^+$ IgD^+ spinal cord-derived B cells at day 7 p.i. were compared to $CD19^+$ IgD^+ B cells isolated from pooled CLN of naive mice or infected mice at day 7 p.i. $CD19^+$ $CD138^+$ ASC and $CD19^+$ IgD^- $CD138^-$ B_{mem} from spinal cords were purified at day 21 p.i. A minimum of 1×10^5 cells were collected per pooled sample and frozen in 400 μl TRIzol (Invitrogen, Carlsbad, CA) at

−80°C for subsequent RNA extraction and PCR analysis, as described previously (29).

Gene expression analysis. Snap-frozen brains or spinal cords from individual mice ($n = 6$ to 7) were placed into TRIzol (Invitrogen, Grand Island, NY) and homogenized by using a TissueLyser and stainless steel beads (Qiagen, Valencia, CA). RNA was extracted according to the manufacturer's instructions. DNA contamination was removed by DNase I treatment for 30 min at 37°C (DNA-free kit; Ambion, Austin, TX), and cDNA was synthesized by using Moloney murine leukemia virus (M-MLV) reverse transcriptase (Invitrogen), oligo(dT) primers (Promega, Madison, WI), and random primers (Promega), as detailed previously (30). Quantitative real-time PCR was performed by using 40 ng of cDNA and SYBR green master mix (Applied Biosystems, Foster City, CA) in duplicate or triplicate on a 7500 Fast real-time PCR system (Applied Biosystems). PCR conditions were 10 min at 95°C followed by 40 cycles at 95°C for 15 s, 60°C for 30 s, and 72°C for 30 s. Primers used for transcripts encoding glyceraldehyde-3-phosphate dehydrogenase (GAPDH), JHMV nucleocapsid, IL-6, IL-10, IL-21, APRIL, CXCL9, CXCL10, CXCL12, BAFF receptor (BAFF-R), B cell maturation antigen (BCMA), and transmembrane activator and calcium modulator and cyclophilin ligand interactor (TACI) were previously described (3, 31). GAPDH, gamma interferon (IFN-γ), BAFF, CCR7, CCL19, CCL21, CXCR3, CXCR4, CXCR5, CXCL13, CD38, IgD, γ heavy chain, and activation-induced cytidine deaminase (AID) mRNA levels were determined by using Applied Biosystems gene expression arrays with Universal TaqMan Fast master mix and TaqMan primers (Applied Biosystems). Primer and probe sequences for κ light chain and sphingosine-1-phosphate 1 (S1P1) mRNA detection were described previously (27, 32). PCR conditions were 20 s at 95°C followed by 40 cycles at 95°C for 3 s and 60°C for 30 s. Transcript levels were calculated relative to the levels of the housekeeping gene GAPDH by using the formula $2^{[CT(\text{GAPDH}) - CT(\text{target gene})]} \times 1{,}000$, where *CT* represents the threshold cycle at which the fluorescent signal becomes significantly higher than that of the background.

Statistical analysis. Gene transcripts in whole spinal cord or brain are expressed as the means ± standard errors of the means (SEM) of values obtained from at least 6 individual mice from 2 separate experiments, each comprising 3 to 4 mice per time point. Flow cytometric analysis data are expressed as the means ± SEM of values from 2 separate experiments, each comprising pooled samples from groups of 3 to 4 mice per time point per experiment. In all cases, a P value of <0.05 was considered significant, as determined by an unpaired t test. Graphs were plotted and statistics were assessed by using GraphPad Prism 4.0 software.

RESULTS

Preferential ASC accumulation in spinal cord correlates with viral persistence independent of total B cells. $CD138^+$ ASC accumulating in the CNS are essential to prevent the reemergence of persisting JHMV infection following T cell-mediated control of infectious virus (20, 23, 24). Furthermore, ASC in spinal cord comprise a larger percentage of total B cells and have a more differentiated MHC class II^- phenotype than do those in brain (10), suggesting preferential accumulation or survival. To better characterize the kinetics of distinct B cell accumulation in brain versus spinal cord, total $CD19^+$ B cells and the $CD138^+$ ASC subset were monitored throughout acute and persistent infection by flow cytometry. B cells were present by as early as day 5 p.i. in brain but were barely detectable in spinal cord. Despite these early differences, B cell numbers peaked at day 7 p.i. in both sites, with overall similar numbers per mg tissue. B cell numbers dropped to comparable levels by days 14 and 21 p.i. but were sustained at higher levels in spinal cords thereafter (Fig. 1A). $CD138^+$ ASC did not emerge until after day 7 p.i., when their numbers increased to maximal levels at between 21 and 28 days p.i. (Fig. 1B). Although numbers of ASC per mg tissue were already slightly elevated in spinal cord relative to brain at day 14 p.i., they were subsequently 4- to 5-fold higher in spinal cords (Fig. 1B). The frequencies of ASC within the total $CD19^+$ B cell population were thus significantly higher in the spinal cord after day 14 p.i., reaching ~50%, versus ~10% in the brain at day 21 p.i. (Fig. 1C). However, while the ASC percentages remained stable in the spinal cord, they continued to increase in the brain through day 42 p.i. Consistent with the increased ASC numbers in the spinal cord, γ heavy chain and κ light chain transcript levels were also significantly higher than those in the brain (Fig. 1D and E). In fact, ~8- to 10-fold differences in transcript levels in comparisons of spinal cord and brain at both days 21 and 35 p.i., but only ~3- to 5-fold differences in ASC numbers, further suggested spinal cord ASC produce more Ab at the cellular level, consistent with enhanced differentiation. A direct correlation between immunoglobulin mRNA and virus-specific Ab was assessed by measuring virus-specific IgG and IgM levels in brain and spinal cord supernatants. Virus-specific IgG and IgM levels were similar at both sites at day 14 p.i. but were higher in spinal cords by day 21 p.i. While IgG levels were significantly increased at both days 21 and 28 p.i., IgM levels were overall lower and most prominently increased in spinal cord at day 28 p.i. (Fig. 1F and G).

Following intracerebral inoculation, JHMV quickly spreads from the brain to the spinal cord, where it preferentially establishes persistence in oligodendrocytes (22). To assess whether preferential accumulation of $CD138^+$ ASC in the spinal cord is associated with increased viral persistence, relative viral loads were compared at both sites throughout infection. Infectious virus titers in spinal cord were higher than those in brain at day 7 p.i. and were controlled with delayed kinetics (Fig. 1H). Consistent with elevated virus titers at day 14 p.i., viral transcript levels were higher in spinal cord than in brain (Fig. 1I). Moreover, although transcript levels gradually declined at both sites, viral transcript levels remained higher in the spinal cord through day 35 p.i. These results suggested that enhanced viral load contributes to preferential accumulation of $CD138^+$ ASC in the spinal cord.

Elevated transcript levels of factors promoting B cell migration, differentiation, and survival correlate with preferential accumulation of ASC in spinal cords. Increased viral load and persistence in the spinal cord relative to the brain may be associated with ongoing immune activation, thereby promoting BBB disruption and/or factors supporting ASC recruitment and survival. Differences in BBB integrity between brain and spinal cord were therefore measured by leakage of NaF administered into the circulation. BBB integrity was significantly compromised at day 7 p.i. in both the brain and spinal cord; however, no differences between each site were detected (Fig. 2A). Furthermore, BBB integrity was largely restored by day 14 p.i. (Fig. 2A). ASC accumulation within the CNS therefore appears to be independent of BBB permeability, regardless of the anatomical site. Differences in tissue-specific expression of factors associated with ASC recruitment and survival were therefore assessed. During JHMV infection, astrocyte-derived CXCL10 drives accumulation of CXCR3-expressing $CD138^+$ ASC in the CNS (33). CXCL10 transcript levels were elevated at day 7 p.i. in both the brain and spinal cord relative to basal levels; however, transcript levels were ~3-fold higher in infected spinal cord than in brain (Fig. 2B). Moreover, although CXCL10 transcript levels declined at both sites, expression levels remained 5- to 10-fold higher in the spinal cord at days 14 and 21 p.i., respectively (Fig. 2B). Similar differences were detected for

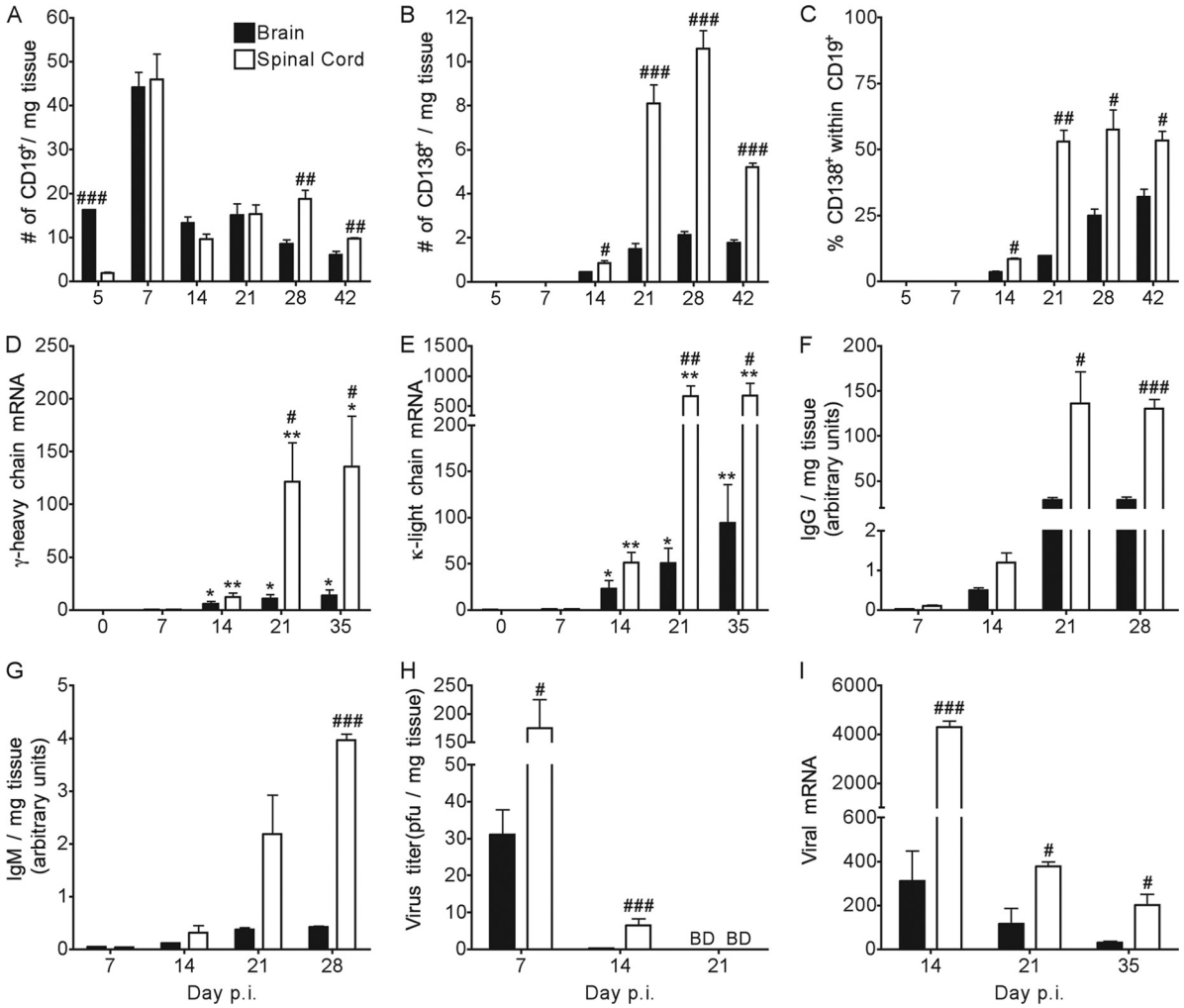

FIG 1 Preferential accumulation of ASC in the spinal cord versus the brain is associated with increased viral loads. (A and B) Numbers of total $CD19^+$ B cells (A) or $CD19^+$ $CD138^+$ ASC (B) were determined by flow cytometry. Data are expressed as the mean number of $CD19^+$ B cells (A) or $CD138^+$ ASC (B) per mg of tissue ± SEM and represent two independent experiments, each comprising pooled brains or spinal cords of 6 to 8 mice per time point. (C) Percentages of $CD138^+$ ASC within total $CD19^+$ B cells calculated as the means ± SEM from data presented in panels A and B. (D and E) Relative transcript levels of γ heavy chain and κ light chain in brains and spinal cords of naive and infected mice assessed by real-time PCR. Data depict the means ± SEM relative to GAPDH mRNA levels for at least 6 to 7 individual mice derived from two independent experiments with at least 3 mice per time point per experiment. Transcript levels at day 7 p.i. are expressed as means ± SEMs relative to GAPDH mRNA levels and were as follows: 0.17 ± 0.08 in brain and 0.26 ± 0.14 in spinal cord for γ heavy chain (D) and 0.8 ± 0.2 in brain and 0.9 ± 0.4 in spinal cord for κ light chain (E). (F and G) Virus-specific IgG2a and IgM levels in clarified supernatants from brain and spinal cord homogenates at the indicated time points were assessed by an ELISA. Arbitrary units reflect Ab levels converted to mg of tissue from 3 to 4 mice per time point. (H) Virus titers in brain or spinal cord supernatants were determined by a plaque assay and are expressed as mean PFU per mg of tissue ± SEM. Data are from two independent experiments with 5 to 10 total mice per time point. (I) Relative transcript levels of viral RNA in brain or spinal cord assessed by real-time PCR. Data depict the means ± SEM relative to GAPDH mRNA levels for 6 to 7 total mice per time point derived from two independent experiments. Significant differences between naive and infected brain or naive and infected spinal cord are indicated (*, $P < 0.05$; **, $P < 0.005$; ***, $P < 0.001$). Significant differences between brain and spinal cord at a given time point are indicated (#, $P < 0.05$; ##, $P < 0.005$; ###, $P < 0.001$). In all cases, a P value of <0.05 was considered significant, as determined by an unpaired t test. BD, below the detection limit.

the IFN-γ-dependent expression of the CXCR3 ligand CXCL9 (Fig. 2C). Consistent with IFN-γ-mediated CXCL9 and CXCL10 upregulation in the CNS during JHMV infection (3), IFN-γ transcript levels were significantly higher in the spinal cord than in the brain (Fig. 2D). These data suggest that enhanced CXCL10 expression in spinal cord relative to that in brain promotes infiltration of $CD138^+$ ASC egressing from lymph nodes at days 14 and 21 p.i.

In addition to chemotaxis, the expression of APRIL and BAFF, key cytokines that promote B cell survival (34–38), may enhance frequencies of $CD138^+$ ASC in the spinal cord. Notably, basal levels of BAFF transcripts were already ~4-fold higher in spinal cord than in brain. At day 7 p.i., BAFF transcript levels were increased ~4- and 2-fold in brain and spinal cord, respectively (Fig. 2E), consistent with IFN-γ-mediated regulation (3, 19). BAFF transcript levels subsequently decreased to background levels in the brain and also gradually declined in spinal cords (Fig. 2E). Overall, BAFF mRNA in the brain remained below basal levels in the spinal cord (Fig. 2E). In contrast to differential basal BAFF expression, APRIL transcript levels in naive mice were similar in both sites and were significantly upregulated only in the spinal

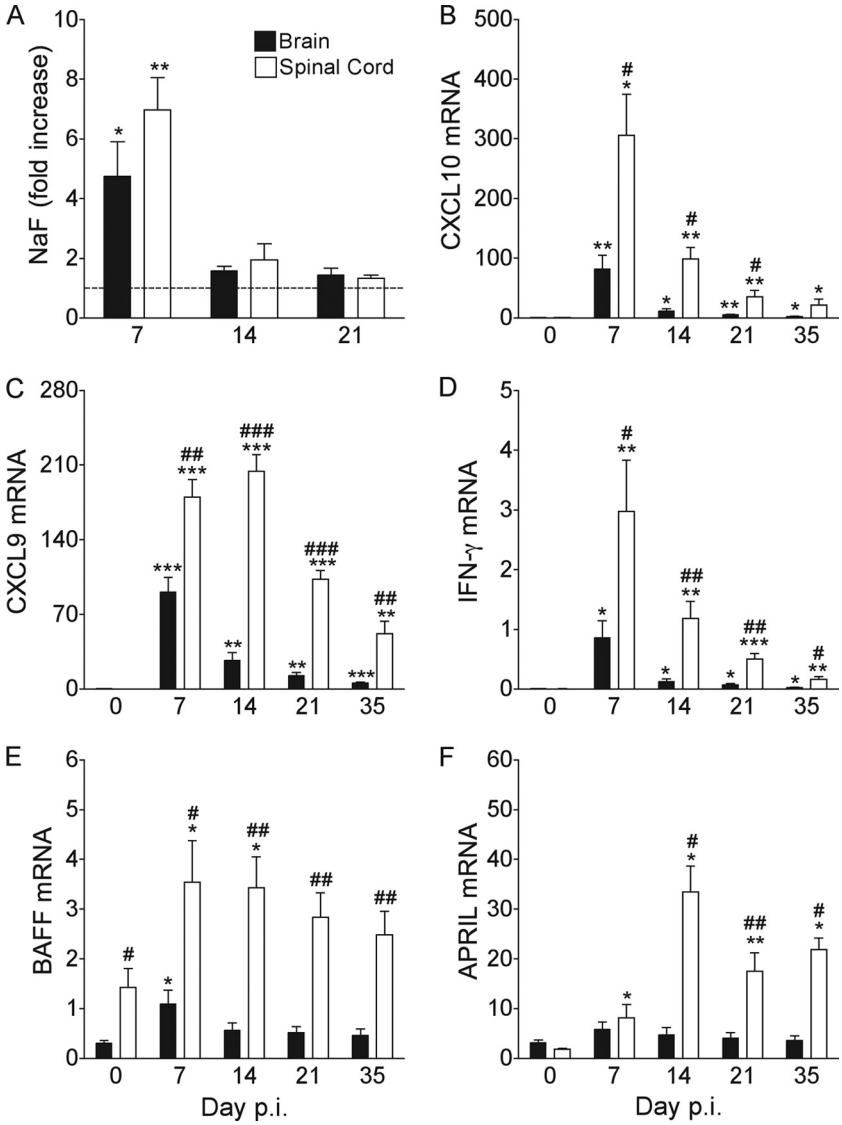

FIG 2 Preferential accumulation of ASC in the spinal cord is associated with enhanced transcript expression of homing and survival factors. (A) BBB permeability changes presented as the mean fold increase in NaF uptake ± SEM measured for at least 6 to 8 individual mice derived from two independent experiments with at least 3 mice per time point per experiment, with levels from uninfected mice set at a value of 1. (B to F) Relative transcript levels of CXCL10, CXCL9, IFN-γ, BAFF, and APRIL in brain and spinal cord of naive and infected mice assessed by real-time PCR. Data depict the means ± SEM relative to GAPDH mRNA levels for at least 6 to 7 individual mice derived from two independent experiments with at least 3 mice per time point per experiment. Significant differences between naive and infected brain or naive and infected spinal cord are indicated (*, $P < 0.05$; **, $P < 0.005$; ***, $P < 0.001$). Significant differences between brain and spinal cord at a given time point are indicated (#, $P < 0.05$; ##, $P < 0.005$; ###, $P < 0.001$). In all cases, a P value of <0.05 was considered significant, as determined by an unpaired t test.

cord (Fig. 2F). Although APRIL transcript levels were already elevated at day 7 p.i., they were increased ~25-fold by day 14 p.i. and remained significantly elevated in the spinal cord relative to the basal expression level through day 35 p.i. (Fig. 2F). These results revealed tissue-specific regulation of both BAFF and APRIL transcripts in the CNS following JHMV infection. Moreover, increased expression levels of transcripts for survival factors in the spinal cord relative to the brain are consistent with a more favorable niche for $CD138^+$ ASC survival.

During persistent JHMV infection, CNS-derived $CD138^+$ ASC initially exhibit an early plasmablast phenotype; however, the gradual loss of MHC class II supports *in situ* differentiation within the CNS or preferential survival of more differentiated ASC (10). In the periphery, ASC differentiation is promoted by the cytokines IL-6, IL-10, and IL-21, which are all expressed in the JHMV-infected CNS (3, 31). We therefore assessed whether increased expression levels of IL-6, IL-10, or IL-21 transcripts in the spinal cord correlated with preferential ASC accumulation. Transcript levels for the T cell-derived cytokines IL-10 and IL-21 peaked by day 7 p.i., coincident with T cell infiltration (39), and subsequently declined but remained above basal levels in both brain and spinal cord through day 21 p.i. (Fig. 3A and B). Nevertheless, IL-10 and IL-21 transcript levels were always significantly higher in spinal cord than in brain, supporting the spinal cord as a pre-

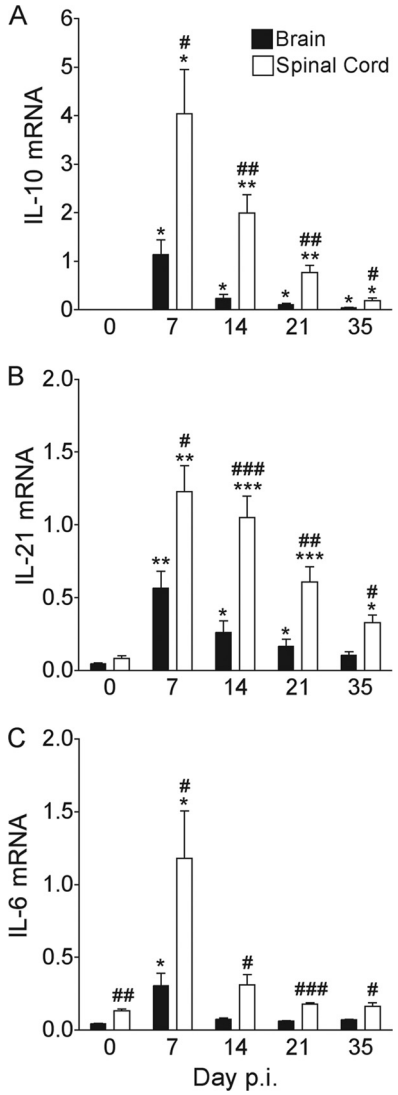

FIG 3 Transcript expression levels of cytokines promoting ASC differentiation are higher in the spinal cord. Relative transcript levels of IL-10, IL-21, and IL-6 in brains and spinal cords of naive and infected mice were assessed by real-time PCR. Data depict the means ± SEM relative to GAPDH mRNA levels for at least 6 to 7 individual mice derived from two independent experiments with at least 3 mice per time point per experiment. Significant differences between naive and infected brain or naive and infected spinal cord are indicated (*, $P < 0.05$; **, $P < 0.005$; ***, $P < 0.001$). Significant differences between brain and spinal cord at a given time point are indicated (#, $P < 0.05$; ##, $P < 0.005$; ###, $P < 0.001$). In all cases, a P value of <0.05 was considered significant, as determined by an unpaired t test.

ferred site of potential ASC differentiation *in situ*. Notably, basal levels of IL-6 transcripts were already ~3-fold higher in spinal cord than in brain (Fig. 3C). While IL-6 transcript levels peaked at day 7 p.i., with expression levels being significantly higher in the spinal cord (Fig. 3), they declined to near-basal levels by day 21 p.i., suggesting a limited contribution of IL-6 to ASC differentiation within the CNS during JHMV persistence.

Decline in levels of early-activated B cells coincides with isotype-switched B_{mem} accumulation. The comparable total $CD19^+$ B cell numbers in brain and spinal cord throughout infection (Fig. 1A), yet preferential accumulation of $CD138^+$ ASC in spinal cords, were consistent with an unbiased recruitment of "bystander" B cells to both sites early during infection. To characterize the phenotype of the $CD138^-$ B cells and potential site-specific alterations in their composition, we assessed surface expression of the B cell receptors IgD and IgM. At day 7 p.i., ~90% of B cells in both the brain and spinal cord were IgD^+ IgM^+ (Fig. 4A and B), consistent with a naive or early-activated phenotype. Although frequencies of IgD^+ IgM^+ B cells declined only slowly by day 14 p.i., they continued to drop more rapidly in the spinal cord thereafter, constituting only ~50% of those in the brain by day 21 p.i. (Fig. 4B). As activated IgD^+ IgM^+ B cells in spleen and lymph nodes are characterized by a downregulation of IgD and sustained IgM expression (40, 41), we monitored IgD expression on CNS-derived B cells over time. Increasing populations of IgD^{lo} IgM^+ (Fig. 4A, dashed ellipse) and IgD^- IgM^+ cells by day 28 p.i. relative to those at day 7 p.i. (Fig. 4A) indicated downregulation of IgD. The frequencies of IgD^{lo} IgM^+ B cells increased to similar levels in both sites (data not shown), consistent with unbiased ongoing recruitment of newly activated B cells from the periphery and/or local activation of already CNS-infiltrated IgD^+ IgM^+ B cells. A similar increase in the frequency of IgD^- IgM^+ B cells to ~20% in both sites (Fig. 4C) yet the enhanced decline of IgD^+ IgM^+ B cells in spinal cord argued against a direct precursor relationship between these CNS populations. With time, the $CD138^-$ B cells also comprised an increasing population lacking both IgD and IgM (Fig. 4D), thus representing isotype-switched antigen-experienced B_{mem}. Although the frequencies of IgD^- IgM^- B_{mem} increased at a similar rate to ~10% and ~15% at both sites by day 14 p.i., accumulation of B_{mem} was accelerated in spinal cord relative to brain by day 21 p.i. (Fig. 4D). The percentages of isotype-switched $CD138^-$ B_{mem} further increased in both sites but remained higher in spinal cord out to day 42 p.i. (Fig. 4D). Overall, the decline in IgD^+ IgM^+ B cells correlated with the increase in the frequency of B_{mem} in both brain and spinal cord but was faster in spinal cord, as noted for ASC.

The majority of virus-specific ASC within the CNS following JHMV infection secrete IgG2a/b (4). The proportion of isotype-switched IgD^- IgM^- B_{mem} in $CD138^-$ B cells (~55%) (Fig. 4D) approximated that of IgG2a/b surface-expressing cells (Fig. 4E), demonstrating that B_{mem} in the CNS largely express IgG2a/b. To further confirm the characteristic phenotype of B_{mem} in expressing surface IgG but limited intracellular IgG, both surface IgG and intracellular IgG were compared in $CD138^-$ B cells and $CD138^+$ ASC (2, 42–44). Intracellular IgG2a/b was detected in <5% of $CD138^-$ B cells but ~55% of $CD138^+$ ASC (Fig. 4E), demonstrating that non-Ab-secreting isotype-switched B_{mem} can localize to the CNS, similarly to ASC. Taken together, the data indicate that naive/early-activated IgD^+ IgM^+ B cells are recruited to brain and spinal cord at similar frequencies early during acute JHMV infection but are progressively replaced by B_{mem} and ASC. This transition is most prominent at between days 14 and 21 p.i., coinciding with the general time of lymph node germinal center formation following infection or immunization (45–49). Furthermore, this process is accelerated at the site of enhanced viral persistence and inflammation, supporting the concept that differentiated B cell accumulation is driven by local chemokines and survival factors.

B cells accumulating early in the spinal cord have an activated phenotype. To further characterize the differentiation state of CNS-localized B cell subsets, spinal cord-derived IgD^+ B cells

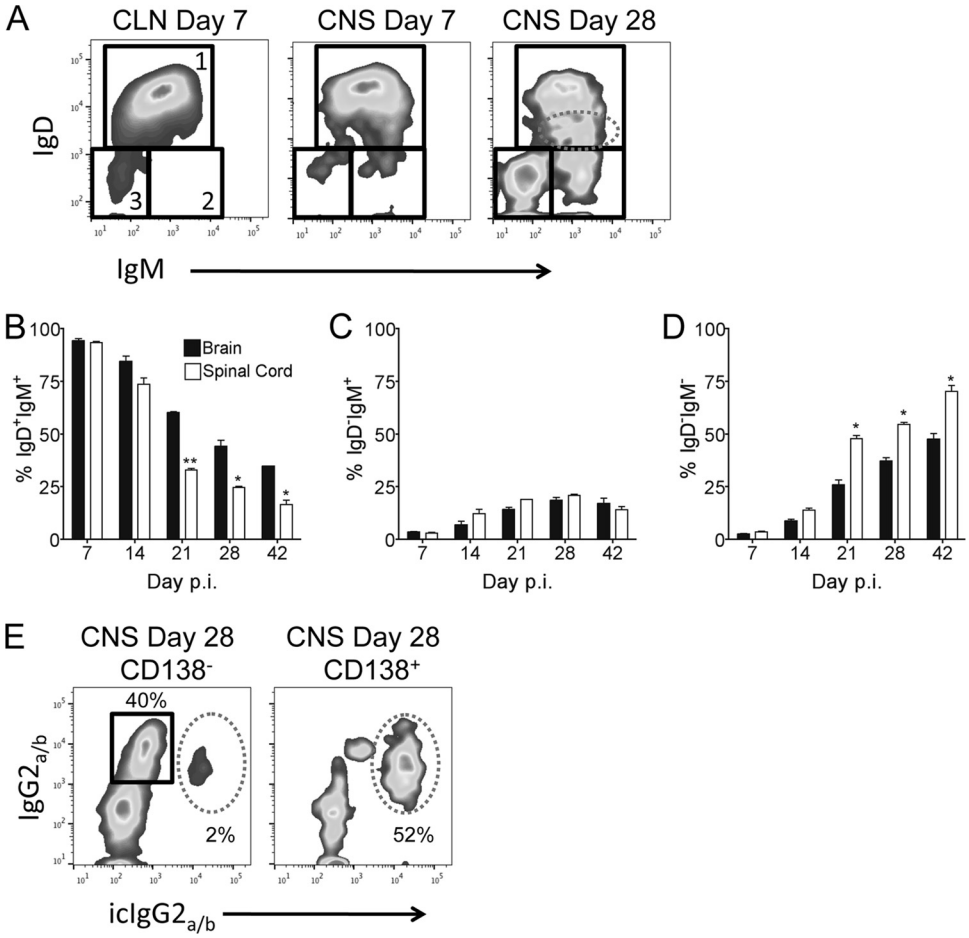

FIG 4 Early-activated B cells are replaced with isotype-switched B_{mem} in the CNS. (A) Representative plots of IgD and IgM expression levels on CLN- and brain-derived CD19$^+$ CD138$^-$ B cells at days 7 and 28 p.i., respectively. Gated populations are indicated as follows: 1, IgD$^+$ IgM$^+$; 2, IgD$^-$ IgM$^+$; 3, IgD$^-$ IgM$^-$. The dashed ellipse represents IgD^{lo} IgM$^+$ B cells. (B to D) Frequencies of IgD$^+$ IgM$^+$ (B), IgD$^-$ IgM$^+$ (C), and IgD$^-$ IgM$^-$ (D) B cells within total CD19$^+$ CD138$^-$ B cells. Data are expressed as the mean percentages of each B cell subset within total CD19$^+$ CD138$^-$ B cells ± SEM and represent two independent experiments, each using pooled brains or spinal cords from 6 to 8 mice per time point. (E) Representative plots of surface IgG2a/b and intracellular IgG2a/b (icIgG2a/b) expression levels by brain CD19$^+$ CD138$^-$ or CD138$^+$ B cells at day 28 p.i. Gated populations are indicated as follows: squares, surface IgG2a/b$^+$ and intracellular IgG2a/b$^-$; dashed ellipses, surface IgG2a/b$^+$ and intracellular IgG2a/b$^+$. Significant differences between brain and spinal cord at a given time point are indicated (*, $P < 0.05$; **, $P < 0.005$). In all cases, a P value of <0.05 was considered significant, as determined by an unpaired t test.

(naive/early activated), IgD$^-$ CD138$^-$ B_{mem}, and CD138$^+$ ASC were monitored for expression of several genes associated with differentiation at days 7 and 21 p.i. Transcript levels in IgD$^+$ B cells purified from CLN of naive mice and mice at day 7 p.i. were used as a reference. Naive mature B cells generally downregulate IgD and CD38 expression following activation in lymphoid organs (40, 41, 50). IgD and CD38 transcript levels were indeed the highest in naive CLN-derived IgD$^+$ B cells and slightly lower at day 7 p.i. In spinal cord-derived IgD$^+$ B cells, IgD transcript levels were ~40-fold lower and CD38 transcripts were 4-fold lower than those in their CLN counterparts (Fig. 5A and B), supporting the concept that the early-arriving IgD$^+$ B cells were activated. As expected, IgD and CD38 transcript levels were comparatively very low in spinal cord-derived CD138$^-$ IgD$^-$ B_{mem} and CD138$^+$ ASC (Fig. 5A and B). A factor that regulates egress of activated lymphocytes from lymphoid tissue is S1P1 (51, 52), predicting that S1P1 transcript levels are lower in spinal cord- than in CLN-derived IgD$^+$ B cells. S1P1 transcript levels were indeed decreased ~4-fold in IgD$^+$ B cells derived from spinal cords at day 7 p.i. compared to naive CLN-derived B cells (Fig. 5C) and were even lower in both B_{mem} and ASC. AID, an enzyme required for immunoglobulin class switching and somatic hypermutation, is upregulated in activated germinal center B cells (53–55). As anticipated, AID transcript levels were elevated ~8-fold in CLN-derived IgD$^+$ B cells at day 7 p.i. relative to the levels in naive counterparts (Fig. 5D), indicating early germinal center reactions. However, AID transcripts were barely detectable in spinal cord-derived IgD$^+$ B cells and undetectable in CD138$^-$ IgD$^-$ B_{mem} and CD138$^+$ ASC (Fig. 5D). These results support that B cells accumulating early in the CNS are derived from activated cells emigrating from the periphery. Moreover, undetectable AID expression levels in early B cells in the spinal cord as well as B_{mem} and ASC accumulating during persistence indicate an absence of local germinal center-type reactivity within the CNS following JHMV infection.

Chemokine and survival factor receptor expression on spinal cord-infiltrating B cell subsets. In the periphery, recently acti-

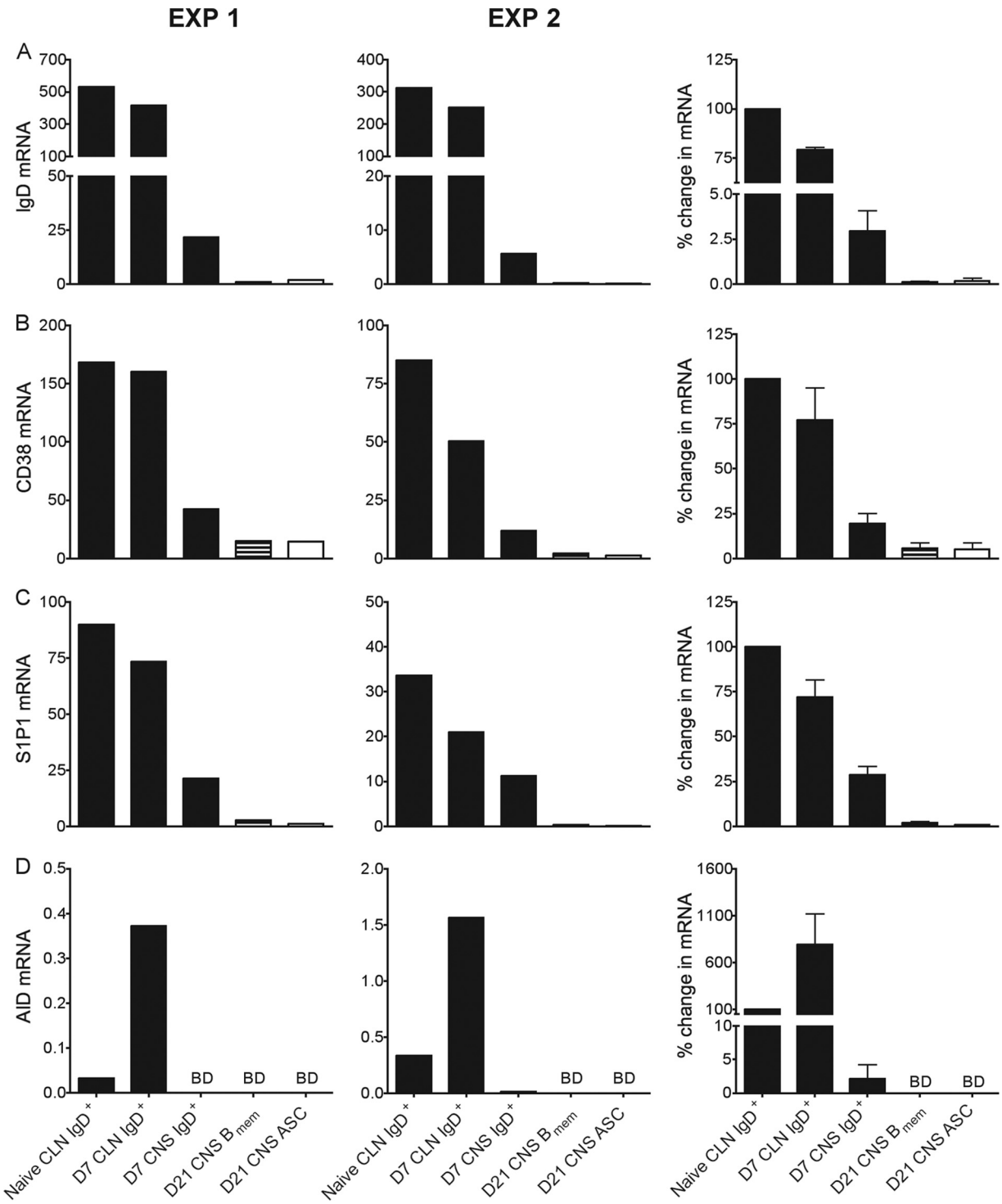

FIG 5 B cells accumulating early in the spinal cord are activated. Relative transcript levels of IgD, CD38, S1P1, and AID in FACS-purified IgD^+ B cells (solid bars), IgD^- $CD138^-$ B_{mem} (striped bars), or $CD138^+$ ASC (empty bars) derived from pooled CLN or spinal cords from 6 to 8 mice per time point per experiment collected at day 0, 7, or 21 p.i. were assessed by real-time PCR. Transcript levels are relative to GAPDH levels. Data from two independent experiments (EXP 1 and EXP 2) are shown. To better reflect relative differences in mRNA levels between populations, data in the last column show the mean percent changes in transcript expression levels of each cell population ± SEM calculated relative to levels of each transcript in naive CLN-derived IgD^+ B cells, which were set to a baseline value of 100. BD, below the detection limit.

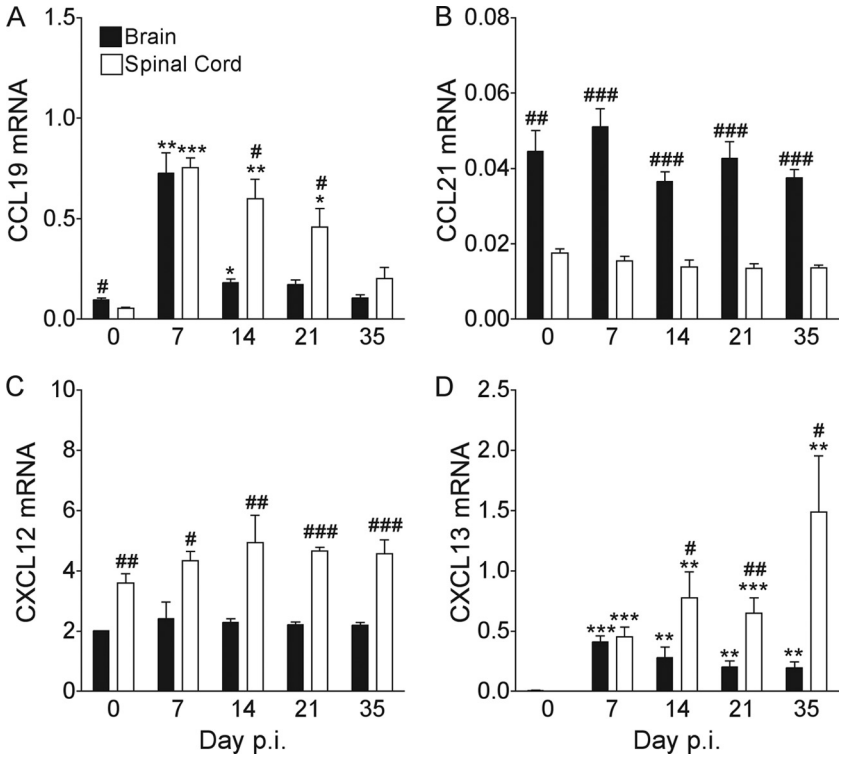

FIG 6 CNS accumulation of early-activated B cells coincides with enhanced transcript expression of lymphoid chemokines. Relative transcript levels of CCL19, CCL21, CXCL12, and CXCL13 in brains and spinal cords of naive and infected mice were assessed by real-time PCR. Data depict the means ± SEM relative to GAPDH mRNA levels for at least 6 to 7 individual mice derived from two independent experiments with at least 3 mice per time point per experiment. Significant differences between naive and infected brain or naive and infected spinal cord are indicated (*, $P < 0.05$; **, $P < 0.005$; ***, $P < 0.001$). Significant differences between brain and spinal cord at a given time point are indicated (#, $P < 0.05$; ##, $P < 0.005$; ###, $P < 0.001$). In all cases, a P value of <0.05 was considered significant, as determined by an unpaired t test.

vated B cells primarily migrate to lymphoid follicles in response to the CXCR5 ligand CXCL13 and the CCR7 ligands CCL19 and CCL21 (56–59). The CXCR4 ligand CXCL12 regulates ASC homing to, and retention in, the bone marrow (60). Detection of transcripts encoding these chemokines in the CNS (14, 33) suggests that they likely play a role in local humoral responses. Expression analysis of these chemokines in brain versus spinal cord revealed that basal CCL19 and CCL21 mRNA expression levels were significantly higher in brains, while CXCL12 transcript levels were significantly higher in spinal cords (Fig. 6A to C). Consistent with data from previous studies (33), CCL19 and CXCL13 transcripts were significantly upregulated at day 7 p.i., with similar expression levels in spinal cord and brain (Fig. 6A and D). Whereas levels of both transcripts declined in brain by day 14 p.i., they remained significantly higher in the spinal cord. In contrast, regardless of the site of infection, neither CCL21 nor CXCL12 transcript levels were altered (Fig. 6B and C). These data suggest that CXCL13 and CCL19 upregulation may contribute to the recruitment of early-activated B cells from the periphery and that their sustained levels in the spinal cord further drive the preferential accumulation of more differentiated B cells. Nevertheless, effects of CXCL12 cannot be excluded, as CXCL12 exerts activities at the BBB by relocation of the chemokine from the luminal to the subluminal space, thereby facilitating leukocyte access to the parenchyma (61, 62).

While ASC migration is regulated by CXCR3 and CXCR4, the chemokine receptors mediating the migration of early-activated B cells into the CNS or other nonlymphoid tissues are unknown to our knowledge. Naive mature B cells primarily express CXCR4, CXCR5, and CCR7, which are retained during initial activation in lymphoid follicles (63). Furthermore, CXCR5 and CCR7 are downregulated and CXCR3 is upregulated during ASC differentiation (64, 65). To assess alterations in chemokine receptors on spinal cord-derived B cell subsets, expression levels of CXCR3, CXCR4, CXCR5, and CCR7 transcripts were compared in IgD^+ B cells, IgD^- $CD138^-$ B_{mem}, and $CD138^+$ ASC. CXCR5 transcripts were expressed at the highest levels in naive and CLN-derived IgD^+ B cells at day 7 p.i. and were ~5-fold reduced in spinal cord-derived IgD^+ B cells (Fig. 7A). Spinal cord-derived IgD^- $CD138^-$ B_{mem} expressed CXCR5 transcripts at levels comparable to those of IgD^+ B cells, but levels were barely detectable in $CD138^+$ ASC (Fig. 7A). CCR7 transcript levels were similar between CLN- and spinal cord-derived IgD^+ B cells and were reduced by ~50% in IgD^- $CD138^-$ B_{mem} (Fig. 7B). As anticipated, CCR7 transcript levels in $CD138^+$ ASC were severely diminished compared to the levels in the other subsets (Fig. 7). Contrasting CXCR5 and CCR7 expression, CXCR4 transcript levels were upregulated by ~5-fold in spinal cord-derived relative to CLN-derived IgD^+ B cells. Moreover, spinal cord-derived IgD^- $CD138^-$ B_{mem} and $CD138^+$ ASC expressed CXCR4 mRNA levels similar to those expressed by naive B cells. Finally, CXCR3 transcript levels were low in both CLN- and spinal cord-derived IgD^+ B cells and highest in spinal cord-derived $CD138^+$ ASC, supporting CXCR3-mediated migration of ASC to the CNS (20, 66). Spinal cord-

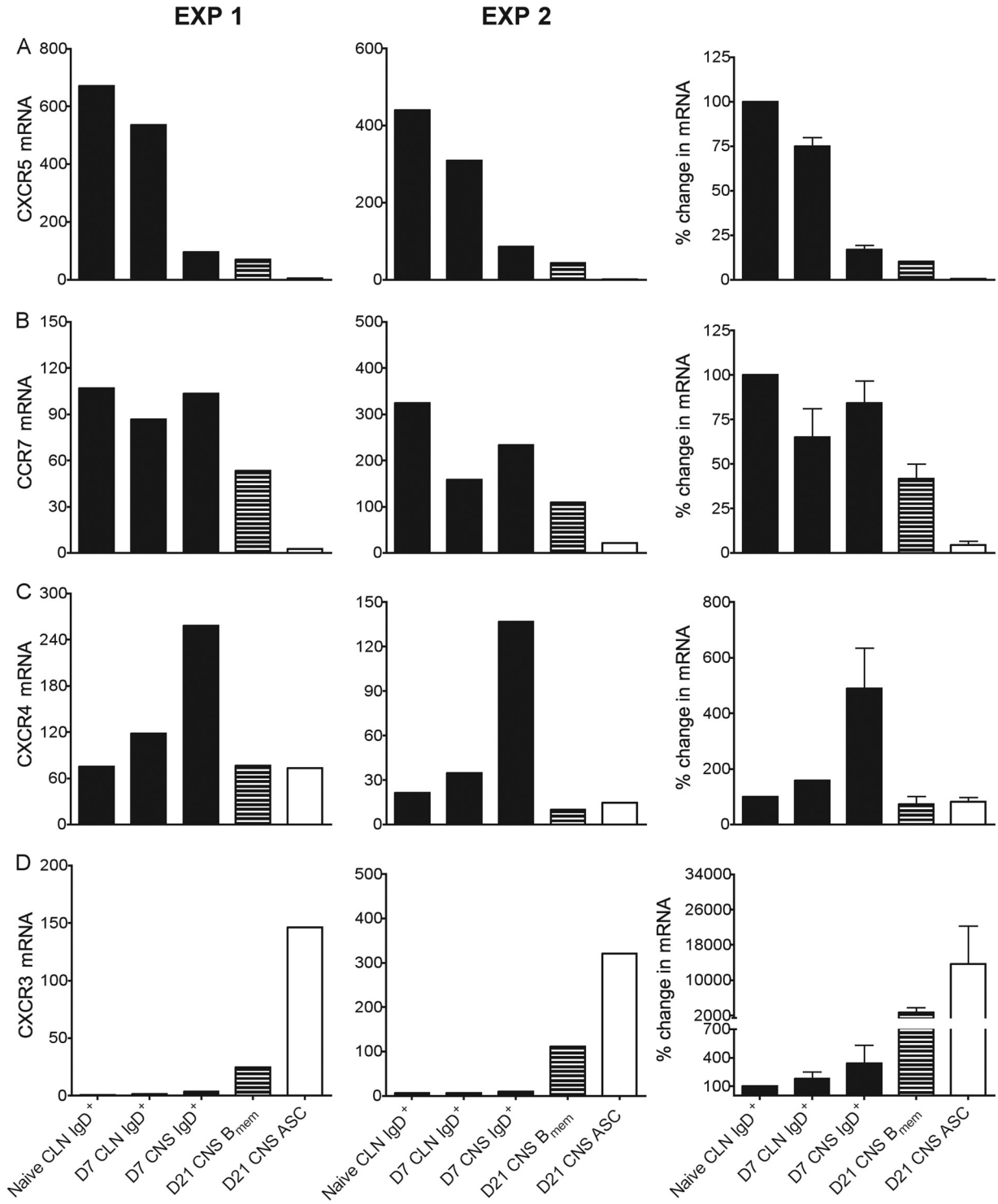

FIG 7 Transcript expression levels of chemokine receptors on spinal cord-derived B cell subsets. Relative transcript levels of CXCR5, CCR7, CXCR4, and CXCR3 in FACS-purified IgD^+ B cells (solid bars), IgD^- $CD138^-$ B_{mem} (striped bars), or $CD138^+$ ASC (empty bars) from pooled CLN or spinal cords of 6 to 8 mice per time point per experiment collected at day 0, 7, or 21 p.i. were assessed by real-time PCR. Transcript levels are relative to GAPDH levels. Two independent experiments (EXP 1 and EXP 2) are shown. To better reflect relative differences in mRNA levels between populations, data in the last column show the mean percent changes in transcript expression levels of each cell population ± SEM calculated relative to levels of each transcript in naive CLN-derived IgD^+ B cells, which were set to a baseline value of 100. BD, below the detection limit.

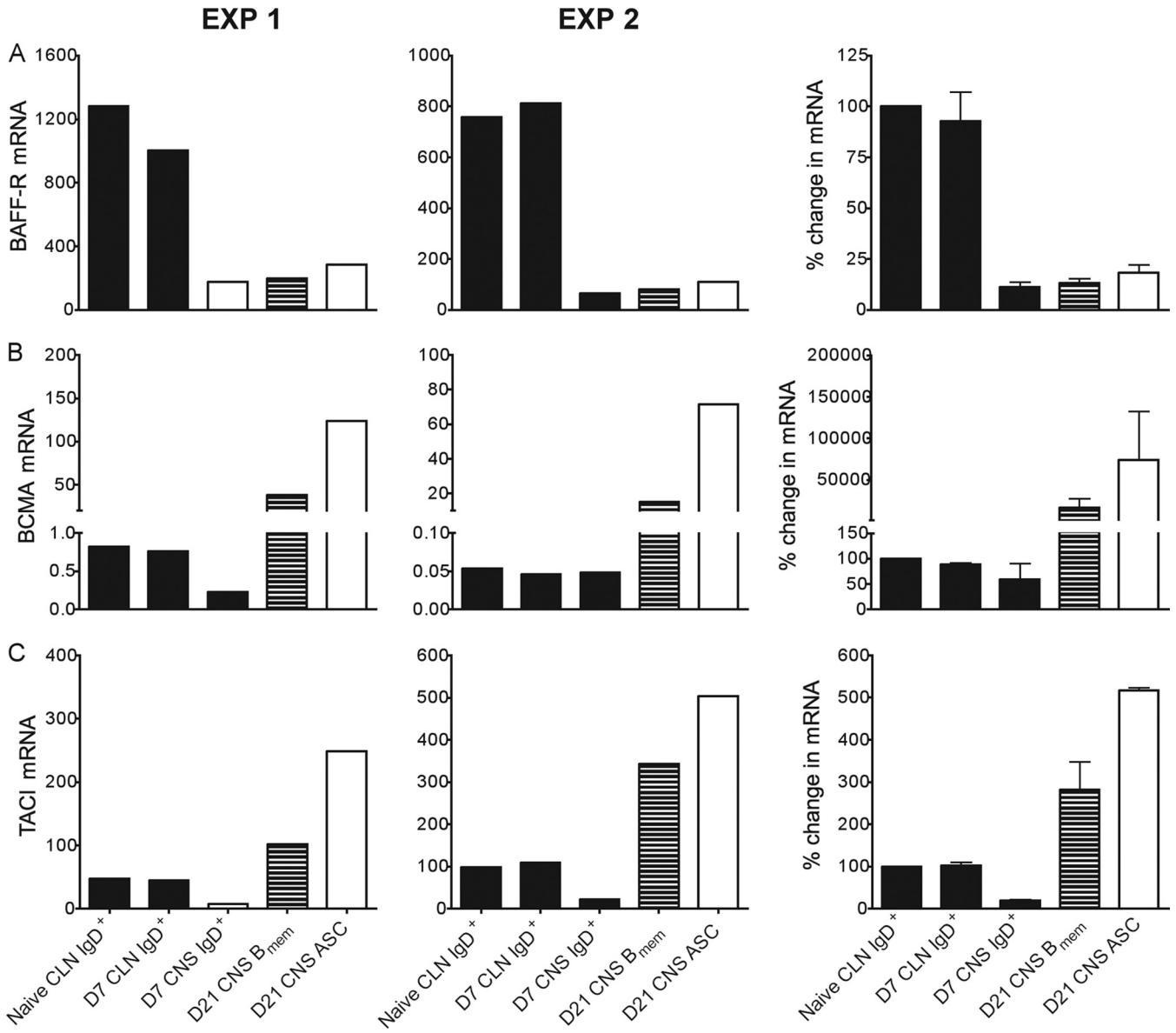

FIG 8 Transcript expression of survival factor receptors in spinal cord-derived B cell subsets. Relative transcript levels of BAFF-R, BCMA, and TACI in FACS-purified IgD^+ B cells (solid bars), IgD^- $CD138^-$ B_{mem} (striped bars), or $CD138^+$ ASC (empty bars) from pooled CLN or spinal cords of 6 to 8 mice collected per time point per experiment at day 0, 7, or 21 p.i. were assessed by real-time PCR. Transcript levels are relative to GAPDH levels. Two independent experiments (EXP 1 and EXP 2) are shown. To better reflect relative differences in mRNA levels between populations, data in the last column show the mean percent changes in transcript expression levels of each cell population ± SEM calculated relative to levels of each transcript in naive CLN-derived IgD^+ B cells, which were set to a baseline value of 100. BD, below the detection limit.

derived IgD^- $CD138^-$ B_{mem} also expressed CXCR3 mRNA albeit at lower levels than in ASC. CCL19/CCL21/CCR7 and/or CXCL12/CXCR4 interactions may thus promote the accumulation of early-activated IgD^+ B cells, while B_{mem} trafficking may be more diversely regulated by responsiveness to CCR7, CXCR4, and CXCR3 signaling.

Distinct B cell subsets are also characterized by differential expression of the B cell survival receptors BCMA, TACI, and BAFF-R. Naive B cells predominantly express BAFF-R, while $CD138^+$ ASC upregulate BCMA and TACI expressions (34, 67–71). Analysis of respective transcripts in B cell subsets in CLN and the spinal cord during JHMV infection revealed that the BAFF-R expression level was highest in CLN-derived IgD^+ B cells, while levels in all three spinal cord-derived populations were ~80% lower (Fig. 8A). On the contrary, spinal cord-derived $CD138^+$ ASC had ~500- and 5-fold-higher BCMA and TACI transcript levels, respectively, than did naive CLN-derived IgD^+ B cells (Fig. 8B and C). Although the BCMA expression level was low in IgD^+ B cells irrespective of their tissue origin, transcript levels for both BAFF-R and TACI were reduced in spinal cord-derived IgD^+ B cells relative to CLN-derived IgD^+ B cells (Fig. 8). B_{mem} revealed an intermediate phenotype, expressing all 3 transcripts at moderate levels. These data suggest that BAFF promotes survival of early-activated IgD^+ B cells within the CNS, while B_{mem} survival

may be regulated by either APRIL or BAFF. Furthermore, the data are consistent with CD138$^+$ ASC receiving TACI- and/or BCMA-dependent survival signals via APRIL engagement.

DISCUSSION

The naive CNS is largely devoid of B cells, but heterogeneous B cell subsets accumulate in cerebrospinal fluid (CSF) during acute and chronic CNS infections (1, 72). However, there is little information on the forces driving CNS B cell lineage accumulation, their heterogeneity, or their function over time. The majority of CSF B cells exhibit an isotype-switched memory phenotype distinct from the dominant naive phenotype in circulation, independent of the disease diagnosis (1). Furthermore, oligoclonal IgG in the CSF during chronic infection as well as MS is consistent with local ASC enrichment (12, 73–75). B cells, including ASC, are also prominent in the CNS during experimental murine infections (2, 10, 20, 76, 77), where they appear to play a protective role (24, 76–79). While CNS-resident ASC may also provide local immunity during human CNS infections (80–83), the influence of other B cell subsets on disease progression in distinct neuroinflammatory infections is unclear. The characterization of B cell accumulation in distinct models is thus critical to reveal potential commonalities, precursor relationships, and humoral-based targets to manipulate distinct B cell functions.

Using the glia-tropic JHMV model of viral encephalomyelitis, here we demonstrate that B cells accumulating in the CNS evolve progressively from an early-activated IgD$^+$ IgM$^+$ phenotype to a more differentiated phenotype comprising IgM$^+$ and IgG$^+$ B$_{mem}$ as well as ASC. Moreover, although overall recruitment kinetics and numbers of total B cells were similar in brain and spinal cord throughout infection, loss of IgD expression, coincident with increased numbers of B$_{mem}$ and CD138$^+$ ASC, was accelerated and more robust in spinal cord after initial T cell-mediated viral control. Early recruitment of IgD$^+$ IgM$^+$ B cells was also noted for Sindbis virus infection (2), suggesting that the mobilization of naive or early-activated B cells prior to the detection of virus-specific ASC in the periphery may be common to a number of viral CNS infections. The data for both models are also consistent with a gradual replacement of early IgD$^+$ B cells in the CNS with more differentiated B cells at the time of peripheral germinal center reactions. Our results also indicate that the magnitude of ongoing inflammatory responses, directly correlating with the extent of viral load, is a dominant force driving preferential recruitment and survival of B$_{mem}$ and ASC at a given anatomical site within the CNS. In this regard, APRIL expression in the spinal cord relative to the brain was not only increased but sustained, indicating distinct site-specific regulation of survival factors in the CNS. Upregulation of APRIL by specific Toll-like receptor (TLR) ligands (84, 85) suggests that enhanced APRIL expression in spinal cord may be attributed to distinct TLR activation. Regardless, elevated viral persistence and tissue damage in the spinal cord relative to brain likely promotes ongoing inflammatory responses and thereby preferential accumulation of more differentiated B cells.

Whether the infiltrating IgD$^+$ IgM$^+$ B cells constitute "early memory" B cells, as indicated during neuroinflammatory diseases in humans (1), is difficult to assess, as murine B$_{mem}$ do not express CD27 (86). Nevertheless, CNS IgD$^+$ IgM$^+$ B cells are presumably activated by innate signals or viral antigen in lymphoid tissue, as naive B cells do not access the human CNS. Modest degrees of activation and migratory behavior to distal sites are supported by the decreased expression levels of IgD, CD38, CXCR5, and S1P1 mRNAs in spinal cord-derived relative to CLN-derived populations in our JHMV model. The chemokines recruiting IgD$^+$ B cells to the CNS are unknown. However, the CCR7 ligands CCL19 and CCL21 are supported as candidates based on the sustained expression of CCR7 and CXCR4 transcripts by IgD$^+$ B cells in our model and the detection of CCR7 on CNS-derived CD19$^+$ B cells during Sindbis virus infection (15). CNS B$_{mem}$ expressed a diverse range of receptors promoting migration, including CCR7, CXCR4, and CXCR3, whereas ASC predominantly expressed CXCR3 and CXCR4. The elevated CXCR3 transcript levels in CNS-derived B$_{mem}$ relative to early-activated IgD$^+$ B cells imply that B$_{mem}$ may respond to CXCR3-mediated signaling, similar to CD138$^+$ ASC during JHMV infection (20, 66).

A potential precursor relationship of early-infiltrating B cells to more differentiated B cells accumulating during CNS virus persistence remains unclear. Although ectopic follicle-like structures sustained by CXCL13 and CCL19/CCL21 have been associated with local B cell differentiation during MS and neuroborreliosis (11, 12, 87, 88), limited or undetectable AID expression in IgD$^+$ B cells, B$_{mem}$, or ASC accumulating within the JHMV-infected CNS argued against local germinal center formation. This is supported by the absence of B cell clusters by histological examination of spinal cords during persistence (10, 20, 33). Similarly, there was no evidence for ectopic follicle formation during Sindbis virus infection (2). The progressive accumulation of more differentiated B cell phenotypes in these two infections is thus more likely driven by the preferential survival of ASC and B$_{mem}$ over IgD$^+$ B cells. Regardless, during persistent JHMV infection, the gradual downregulation of MHC class II on ASC supports their ongoing focal differentiation (10). It thus remains possible that ASC and B$_{mem}$ continue to proliferate and differentiate locally within the CNS. In this context, it is of interest to note that B$_{mem}$ may convert to ASC in the presence of CXCL10, thus potentially contributing to long-lived ASC even in the absence of antigen restimulation (89).

While ASC appear to mediate protective functions by controlling persistent virus, the functions of heterologous B cell subsets within the infected CNS are unknown. Besides serving as precursors to more differentiated B$_{mem}$ or ASC, they may participate as antigen-presenting cells (APC) for T cell activation or exert protective functions via cytokine secretion (90–96). In the JHMV model, B cell-deficient and B cell-sufficient, yet Ab-deficient, mice provided no evidence for a role of B cells in APC function (24, 25). Nevertheless, B cells play an Ab-independent role as APC in graft rejection and the experimental allergic encephalomyelitis model of MS (96–98), thereby playing detrimental roles. Taken together, both JHMV and Sindbis virus infection models demonstrate commonalities in B cell subset recruitment and dynamics. Moreover, this is the first study to reveal that virus load drives enrichment of B$_{mem}$ and antiviral ASC in a nonlymphoid organ.

ACKNOWLEDGMENT

This work was supported by U.S. National Institutes of Health grants NS086299 and AI047249.

REFERENCES

1. **Cepok S, von Geldern G, Grummel V, Hochgesand S, Celik H, Hartung H, Hemmer B.** 2006. Accumulation of class switched IgD-IgM- memory B cells in the cerebrospinal fluid during neuroinflammation. J. Neuroimmunol. **180:**33–39. http://dx.doi.org/10.1016/j.jneuroim.2006.06.031.

2. **Metcalf TU, Griffin DE.** 2011. Alphavirus-induced encephalomyelitis: antibody-secreting cells and viral clearance from the nervous system. J. Virol. **85:**11490–11501. http://dx.doi.org/10.1128/JVI.05379-11.
3. **Phares TW, Marques CP, Stohlman SA, Hinton DR, Bergmann CC.** 2011. Factors supporting intrathecal humoral responses following viral encephalomyelitis. J. Virol. **85:**2589–2598. http://dx.doi.org/10.1128/JVI.02260-10.
4. **Tschen SI, Bergmann CC, Ramakrishna C, Morales S, Atkinson R, Stohlman SA.** 2002. Recruitment kinetics and composition of antibody-secreting cells within the central nervous system following viral encephalomyelitis. J. Immunol. **168:**2922–2929. http://dx.doi.org/10.4049/jimmunol.168.6.2922.
5. **Ankeny DP, Guan Z, Popovich PG.** 2009. B cells produce pathogenic antibodies and impair recovery after spinal cord injury in mice. J. Clin. Invest. **119:**2990–2999. http://dx.doi.org/10.1172/JCI39780.
6. **Pohl-Koppe A, Kaiser R, Meulen VT, Liebert UG.** 1995. Antibody reactivity to individual structural proteins of measles virus in the CSF of SSPE and MS patients. Clin. Diagn. Virol. **4:**135–147. http://dx.doi.org/10.1016/0928-0197(95)00006-T.
7. **Norrby E, Link H.** 1977. The relationship between measles virus-specific antibodies and oligoclonal IgG in the cerebrospinal fluid from patients with subacute sclerosing panencephalitis and multiple sclerosis. Acta Neurol. Scand. Suppl. **63:**161–171.
8. **Owens GP, Ritchie AM, Burgoon MP, Williamson RA, Corboy JR, Gilden DH.** 2003. Single-cell repertoire analysis demonstrates that clonal expansion is a prominent feature of the B cell response in multiple sclerosis cerebrospinal fluid. J. Immunol. **171:**2725–2733. http://dx.doi.org/10.4049/jimmunol.171.5.2725.
9. **Burgoon MP, Caldas YA, Keays KM, Yu X, Gilden DH, Owens GP.** 2006. Recombinant antibodies generated from both clonal and less abundant plasma cell immunoglobulin G sequences in subacute sclerosing panencephalitis brain are directed against measles virus. J. Neurovirol. **12:**398–402. http://dx.doi.org/10.1080/13550280600957414.
10. **Tschen SI, Stohlman SA, Ramakrishna C, Hinton DR, Atkinson RD, Bergmann CC.** 2006. CNS viral infection diverts homing of antibody-secreting cells from lymphoid organs to the CNS. Eur. J. Immunol. **36:**603–612. http://dx.doi.org/10.1002/eji.200535123.
11. **Serafini B, Rosicarelli B, Magliozzi R, Stigliano E, Aloisi F.** 2004. Detection of ectopic B-cell follicles with germinal centers in the meninges of patients with secondary progressive multiple sclerosis. Brain Pathol. **14:**164–174. http://dx.doi.org/10.1111/j.1750-3639.2004.tb00049.x.
12. **Narayan K, Dail D, Li L, Cadavid D, Amrute S, Fitzgerald-Bocarsly P, Pachner AR.** 2005. The nervous system as ectopic germinal center: CXCL13 and IgG in Lyme neuroborreliosis. Ann. Neurol. **57:**813–823. http://dx.doi.org/10.1002/ana.20486.
13. **Corcione A, Aloisi F, Serafini B, Capello E, Mancardi GL, Pistoia V, Uccelli A.** 2005. B-cell differentiation in the CNS of patients with multiple sclerosis. Autoimmun. Rev. **4:**549–554. http://dx.doi.org/10.1016/j.autrev.2005.04.012.
14. **Lalor SJ, Segal BM.** 2010. Lymphoid chemokines in the CNS. J. Neuroimmunol. **224:**56–61. http://dx.doi.org/10.1016/j.jneuroim.2010.05.017.
15. **Metcalf TU, Baxter VK, Nilaratanakul V, Griffin DE.** 2013. Recruitment and retention of B cells in the central nervous system in response to alphavirus encephalomyelitis. J. Virol. **87:**2420–2429. http://dx.doi.org/10.1128/JVI.01769-12.
16. **Kowarik MC, Cepok S, Sellner J, Grummel V, Weber MS, Korn T, Berthele A, Hemmer B.** 2012. CXCL13 is the major determinant for B cell recruitment to the CSF during neuroinflammation. J. Neuroinflammation **9:**93. http://dx.doi.org/10.1186/1742-2094-9-93.
17. **Magliozzi R, Columba-Cabezas S, Serafini B, Aloisi F.** 2004. Intracerebral expression of CXCL13 and BAFF is accompanied by formation of lymphoid follicle-like structures in the meninges of mice with relapsing experimental autoimmune encephalomyelitis. J. Neuroimmunol. **148:**11–23. http://dx.doi.org/10.1016/j.jneuroim.2003.10.056.
18. **Thangarajh M, Masterman T, Hillert J, Moerk S, Jonsson R.** 2007. A proliferation-inducing ligand (APRIL) is expressed by astrocytes and is increased in multiple sclerosis. Scand. J. Immunol. **65:**92–98. http://dx.doi.org/10.1111/j.1365-3083.2006.01867.x.
19. **Krumbholz M, Theil D, Derfuss T, Rosenwald A, Schrader F, Monoranu CM, Kalled SL, Hess DM, Serafini B, Aloisi F, Wekerle H, Hohlfeld R, Meinl E.** 2005. BAFF is produced by astrocytes and up-regulated in multiple sclerosis lesions and primary central nervous system lymphoma. J. Exp. Med. **201:**195–200. http://dx.doi.org/10.1084/jem.20041674.
20. **Marques CP, Kapil P, Hinton DR, Hindinger C, Nutt SL, Ransohoff RM, Phares TW, Stohlman SA, Bergmann CC.** 2011. CXCR3-dependent plasma blast migration to the central nervous system during viral encephalomyelitis. J. Virol. **85:**6136–6147. http://dx.doi.org/10.1128/JVI.00202-11.
21. **Wang FI, Hinton DR, Gilmore W, Trousdale MD, Fleming JO.** 1992. Sequential infection of glial cells by the murine hepatitis virus JHM strain (MHV-4) leads to a characteristic distribution of demyelination. Lab. Invest. **66:**744–754.
22. **Parra B, Hinton DR, Marten NW, Bergmann CC, Lin MT, Yang CS, Stohlman SA.** 1999. IFN-gamma is required for viral clearance from central nervous system oligodendroglia. J. Immunol. **162:**1641–1647.
23. **Bergmann CC, Lane TE, Stohlman SA.** 2006. Coronavirus infection of the central nervous system: host-virus stand-off. Nat. Rev. Microbiol. **4:**121–132. http://dx.doi.org/10.1038/nrmicro1343.
24. **Ramakrishna C, Bergmann CC, Atkinson R, Stohlman SA.** 2003. Control of central nervous system viral persistence by neutralizing antibody. J. Virol. **77:**4670–4678. http://dx.doi.org/10.1128/JVI.77.8.4670-4678.2003.
25. **Ramakrishna C, Stohlman SA, Atkinson RD, Shlomchik MJ, Bergmann CC.** 2002. Mechanisms of central nervous system viral persistence: the critical role of antibody and B cells. J. Immunol. **168:**1204–1211. http://dx.doi.org/10.4049/jimmunol.168.3.1204.
26. **Fleming JO, Trousdale MD, el-Zaatari FA, Stohlman SA, Weiner LP.** 1986. Pathogenicity of antigenic variants of murine coronavirus JHM selected with monoclonal antibodies. J. Virol. **58:**869–875.
27. **Phares TW, Kean RB, Mikheeva T, Hooper DC.** 2006. Regional differences in blood-brain barrier permeability changes and inflammation in the apathogenic clearance of virus from the central nervous system. J. Immunol. **176:**7666–7675. http://dx.doi.org/10.4049/jimmunol.176.12.7666.
28. **Bergmann CC, Altman JD, Hinton D, Stohlman SA.** 1999. Inverted immunodominance and impaired cytolytic function of CD8+ T cells during viral persistence in the central nervous system. J. Immunol. **163:**3379–3387.
29. **Ireland DD, Stohlman SA, Hinton DR, Kapil P, Silverman RH, Atkinson RA, Bergmann CC.** 2009. RNase L mediated protection from virus induced demyelination. PLoS Pathog. **5:**e1000602. http://dx.doi.org/10.1371/journal.ppat.1000602.
30. **de Aquino MT, Puntambekar SS, Savarin C, Bergmann CC, Phares TW, Hinton DR, Stohlman SA.** 2013. Role of CD25(+) CD4(+) T cells in acute and persistent coronavirus infection of the central nervous system. Virology **447:**112–120. http://dx.doi.org/10.1016/j.virol.2013.08.030.
31. **Puntambekar SS, Bergmann CC, Savarin C, Karp CL, Phares TW, Parra GI, Hinton DR, Stohlman SA.** 2011. Shifting hierarchies of interleukin-10-producing T cell populations in the central nervous system during acute and persistent viral encephalomyelitis. J. Virol. **85:**6702–6713. http://dx.doi.org/10.1128/JVI.00200-11.
32. **Matloubian M, Lo CG, Cinamon G, Lesneski MJ, Xu Y, Brinkmann V, Allende ML, Proia RL, Cyster JG.** 2004. Lymphocyte egress from thymus and peripheral lymphoid organs is dependent on S1P receptor 1. Nature **427:**355–360. http://dx.doi.org/10.1038/nature02284.
33. **Phares TW, Stohlman SA, Hinton DR, Bergmann CC.** 2013. Astrocyte-derived CXCL10 drives accumulation of antibody-secreting cells in the central nervous system during viral encephalomyelitis. J. Virol. **87:**3382–3392. http://dx.doi.org/10.1128/JVI.03307-12.
34. **Benson MJ, Dillon SR, Castigli E, Geha RS, Xu S, Lam KP, Noelle RJ.** 2008. Cutting edge: the dependence of plasma cells and independence of memory B cells on BAFF and APRIL. J. Immunol. **180:**3655–3659. http://dx.doi.org/10.4049/jimmunol.180.6.3655.
35. **Bossen C, Cachero TG, Tardivel A, Ingold K, Willen L, Dobles M, Scott ML, Maquelin A, Belnoue E, Siegrist CA, Chevrier S, Acha-Orbea H, Leung H, Mackay F, Tschopp J, Schneider P.** 2008. TACI, unlike BAFF-R, is solely activated by oligomeric BAFF and APRIL to support survival of activated B cells and plasmablasts. Blood **111:**1004–1012. http://dx.doi.org/10.1182/blood-2007-09-110874.
36. **Belnoue E, Pihlgren M, McGaha TL, Tougne C, Rochat AF, Bossen C, Schneider P, Huard B, Lambert PH, Siegrist CA.** 2008. APRIL is critical for plasmablast survival in the bone marrow and poorly expressed by early-life bone marrow stromal cells. Blood **111:**2755–2764. http://dx.doi.org/10.1182/blood-2007-09-110858.

37. **Cassese G, Arce S, Hauser AE, Lehnert K, Moewes B, Mostarac M, Muehlinghaus G, Szyska M, Radbruch A, Manz RA.** 2003. Plasma cell survival is mediated by synergistic effects of cytokines and adhesion-dependent signals. J. Immunol. **171:**1684–1690. http://dx.doi.org/10.4049/jimmunol.171.4.1684.
38. **Rolink AG, Tschopp J, Schneider P, Melchers F.** 2002. BAFF is a survival and maturation factor for mouse B cells. Eur. J. Immunol. **32:**2004–2010. http://dx.doi.org/10.1002/1521-4141(200207)32:7<2004::AID-IMMU2004>3.0.CO;2-5.
39. **Savarin C, Stohlman SA, Atkinson R, Ransohoff RM, Bergmann CC.** 2010. Monocytes regulate T cell migration through the glia limitans during acute viral encephalitis. J. Virol. **84:**4878–4888. http://dx.doi.org/10.1128/JVI.00051-10.
40. **Bourgois A, Kitajima K, Hunter IR, Askonas BA.** 1977. Surface immunoglobulins of lipopolysaccharide-stimulated spleen cells. The behavior of IgM, IgD and IgG. Eur. J. Immunol. **7:**151–153.
41. **Monroe JG, Havran WL, Cambier JC.** 1983. B lymphocyte activation: entry into cell cycle is accompanied by decreased expression of IgD but not IgM. Eur. J. Immunol. **13:**208–213. http://dx.doi.org/10.1002/eji.1830130306.
42. **Arpin C, Dechanet J, Van Kooten C, Merville P, Grouard G, Briere F, Banchereau J, Liu YJ.** 1995. Generation of memory B cells and plasma cells in vitro. Science **268:**720–722. http://dx.doi.org/10.1126/science.7537388.
43. **Tangye SG, Avery DT, Hodgkin PD.** 2003. A division-linked mechanism for the rapid generation of Ig-secreting cells from human memory B cells. J. Immunol. **170:**261–269. http://dx.doi.org/10.4049/jimmunol.170.1.261.
44. **Blink EJ, Light A, Kallies A, Nutt SL, Hodgkin PD, Tarlinton DM.** 2005. Early appearance of germinal center-derived memory B cells and plasma cells in blood after primary immunization. J. Exp. Med. **201:**545–554. http://dx.doi.org/10.1084/jem.20042060.
45. **Jacob J, Kassir R, Kelsoe G.** 1991. In situ studies of the primary immune response to (4-hydroxy-3-nitrophenyl)acetyl. I. The architecture and dynamics of responding cell populations. J. Exp. Med. **173:**1165–1175.
46. **MacLennan IC.** 1994. Germinal centers. Annu. Rev. Immunol. **12:**117–139. http://dx.doi.org/10.1146/annurev.iy.12.040194.001001.
47. **Rasheed MA, Latner DR, Aubert RD, Gourley T, Spolski R, Davis CW, Langley WA, Ha SJ, Ye L, Sarkar S, Kalia V, Konieczny BT, Leonard WJ, Ahmed R.** 2013. Interleukin-21 is a critical cytokine for the generation of virus-specific long-lived plasma cells. J. Virol. **87:**7737–7746. http://dx.doi.org/10.1128/JVI.00063-13.
48. **Olson MR, McDermott DS, Varga SM.** 2012. The initial draining lymph node primes the bulk of the CD8 T cell response and influences memory T cell trafficking after a systemic viral infection. PLoS Pathog. **8:**e1003054. http://dx.doi.org/10.1371/journal.ppat.1003054.
49. **Boyden AW, Legge KL, Waldschmidt TJ.** 2012. Pulmonary infection with influenza A virus induces site-specific germinal center and T follicular helper cell responses. PLoS One **7:**e40733. http://dx.doi.org/10.1371/journal.pone.0040733.
50. **Oliver AM, Martin F, Kearney JF.** 1997. Mouse CD38 is down-regulated on germinal center B cells and mature plasma cells. J. Immunol. **158:**1108–1115.
51. **Chiba K, Matsuyuki H, Maeda Y, Sugahara K.** 2006. Role of sphingosine 1-phosphate receptor type 1 in lymphocyte egress from secondary lymphoid tissues and thymus. Cell. Mol. Immunol. **3:**11–19. http://www.cmi.ustc.edu.cn/3/1/11.pdf.
52. **Schwab SR, Cyster JG.** 2007. Finding a way out: lymphocyte egress from lymphoid organs. Nat. Immunol. **8:**1295–1301. http://dx.doi.org/10.1038/ni1545.
53. **Keim C, Kazadi D, Rothschild G, Basu U.** 2013. Regulation of AID, the B-cell genome mutator. Genes Dev. **27:**1–17. http://dx.doi.org/10.1101/gad.200014.112.
54. **Maul RW, Gearhart PJ.** 2010. AID and somatic hypermutation. Adv. Immunol. **105:**159–191. http://dx.doi.org/10.1016/S0065-2776(10)05006-6.
55. **Muramatsu M, Kinoshita K, Fagarasan S, Yamada S, Shinkai Y, Honjo T.** 2000. Class switch recombination and hypermutation require activation-induced cytidine deaminase (AID), a potential RNA editing enzyme. Cell **102:**553–563. http://dx.doi.org/10.1016/S0092-8674(00)00078-7.
56. **Okada T, Ngo VN, Ekland EH, Forster R, Lipp M, Littman DR, Cyster JG.** 2002. Chemokine requirements for B cell entry to lymph nodes and Peyer's patches. J. Exp. Med. **196:**65–75. http://dx.doi.org/10.1084/jem.20020201.
57. **Forster R, Schubel A, Breitfeld D, Kremmer E, Renner-Muller I, Wolf E, Lipp M.** 1999. CCR7 coordinates the primary immune response by establishing functional microenvironments in secondary lymphoid organs. Cell **99:**23–33. http://dx.doi.org/10.1016/S0092-8674(00)80059-8.
58. **Ansel KM, Ngo VN, Hyman PL, Luther SA, Forster R, Sedgwick JD, Browning JL, Lipp M, Cyster JG.** 2000. A chemokine-driven positive feedback loop organizes lymphoid follicles. Nature **406:**309–314. http://dx.doi.org/10.1038/35018581.
59. **Forster R, Mattis AE, Kremmer E, Wolf E, Brem G, Lipp M.** 1996. A putative chemokine receptor, BLR1, directs B cell migration to defined lymphoid organs and specific anatomic compartments of the spleen. Cell **87:**1037–1047. http://dx.doi.org/10.1016/S0092-8674(00)81798-5.
60. **Cyster JG.** 2003. Homing of antibody secreting cells. Immunol. Rev. **194:**48–60. http://dx.doi.org/10.1034/j.1600-065X.2003.00041.x.
61. **Cruz-Orengo L, Holman DW, Dorsey D, Zhou L, Zhang P, Wright M, McCandless EE, Patel JR, Luker GD, Littman DR, Russell JH, Klein RS.** 2011. CXCR7 influences leukocyte entry into the CNS parenchyma by controlling abluminal CXCL12 abundance during autoimmunity. J. Exp. Med. **208:**327–339. http://dx.doi.org/10.1084/jem.20102010.
62. **McCandless EE, Budde M, Lees JR, Dorsey D, Lyng E, Klein RS.** 2009. IL-1R signaling within the central nervous system regulates CXCL12 expression at the blood-brain barrier and disease severity during experimental autoimmune encephalomyelitis. J. Immunol. **183:**613–620. http://dx.doi.org/10.4049/jimmunol.0802258.
63. **Cyster JG.** 2005. Chemokines, sphingosine-1-phosphate, and cell migration in secondary lymphoid organs. Annu. Rev. Immunol. **23:**127–159. http://dx.doi.org/10.1146/annurev.immunol.23.021704.115628.
64. **Pereira JP, Kelly LM, Cyster JG.** 2010. Finding the right niche: B-cell migration in the early phases of T-dependent antibody responses. Int. Immunol. **22:**413–419. http://dx.doi.org/10.1093/intimm/dxq047.
65. **Goodnow CC, Vinuesa CG, Randall KL, Mackay F, Brink R.** 2010. Control systems and decision making for antibody production. Nat. Immunol. **11:**681–688. http://dx.doi.org/10.1038/ni.1900.
66. **Gil-Cruz C, Perez-Shibayama C, Firner S, Waisman A, Bechmann I, Thiel V, Cervantes-Barragan L, Ludewig B.** 2012. T helper cell- and CD40-dependent germline IgM prevents chronic virus-induced demyelinating disease. Proc. Natl. Acad. Sci. U. S. A. **109:**1233–1238. http://dx.doi.org/10.1073/pnas.1115154109.
67. **Mackay F, Schneider P, Rennert P, Browning J.** 2003. BAFF and APRIL: a tutorial on B cell survival. Annu. Rev. Immunol. **21:**231–264. http://dx.doi.org/10.1146/annurev.immunol.21.120601.141152.
68. **Rauch M, Tussiwand R, Bosco N, Rolink AG.** 2009. Crucial role for BAFF-BAFF-R signaling in the survival and maintenance of mature B cells. PLoS One **4:**e5456. http://dx.doi.org/10.1371/journal.pone.0005456.
69. **Shulga-Morskaya S, Dobles M, Walsh ME, Ng LG, MacKay F, Rao SP, Kalled SL, Scott ML.** 2004. B cell-activating factor belonging to the TNF family acts through separate receptors to support B cell survival and T cell-independent antibody formation. J. Immunol. **173:**2331–2341. http://dx.doi.org/10.4049/jimmunol.173.4.2331.
70. **Mantchev GT, Cortesao CS, Rebrovich M, Cascalho M, Bram RJ.** 2007. TACI is required for efficient plasma cell differentiation in response to T-independent type 2 antigens. J. Immunol. **179:**2282–2288. http://dx.doi.org/10.4049/jimmunol.179.4.2282.
71. **O'Connor BP, Raman VS, Erickson LD, Cook WJ, Weaver LK, Ahonen C, Lin LL, Mantchev GT, Bram RJ, Noelle RJ.** 2004. BCMA is essential for the survival of long-lived bone marrow plasma cells. J. Exp. Med. **199:**91–98. http://dx.doi.org/10.1084/jem.20031330.
72. **Corcione A, Casazza S, Ferretti E, Giunti D, Zappia E, Pistorio A, Gambini C, Mancardi GL, Uccelli A, Pistoia V.** 2004. Recapitulation of B cell differentiation in the central nervous system of patients with multiple sclerosis. Proc. Natl. Acad. Sci. U. S. A. **101:**11064–11069. http://dx.doi.org/10.1073/pnas.0402455101.
73. **Skoldenberg B, Kalimo K, Carlstrom A, Forsgren M, Halonen P.** 1981. Herpes simplex encephalitis: a serological follow-up study. Synthesis of herpes simplex virus immunoglobulin M, A, and G antibodies and development of oligoclonal immunoglobulin G in the central nervous system. Acta Neurol. Scand. **63:**273–285.
74. **Schultze D, Weder B, Cassinotti P, Vitek L, Krausse K, Fierz W.** 2004. Diagnostic significance of intrathecally produced herpes simplex and varizella-zoster virus-specific antibodies in central nervous system infections. Swiss Med. Wkly. **134:**700–704. http://www.smw.ch/docs/pdf200x/2004/47/smw-10766.pdf.
75. **Burke DS, Nisalak A, Lorsomrudee W, Ussery MA, Laorpongse T.** 1985.

Virus-specific antibody-producing cells in blood and cerebrospinal fluid in acute Japanese encephalitis. J. Med. Virol. **17:**283–292. http://dx.doi.org/10.1002/jmv.1890170310.

76. **Griffin D, Levine B, Tyor W, Ubol S, Despres P.** 1997. The role of antibody in recovery from alphavirus encephalitis. Immunol. Rev. **159:**155–161. http://dx.doi.org/10.1111/j.1600-065X.1997.tb01013.x.
77. **Hooper DC, Phares TW, Fabis MJ, Roy A.** 2009. The production of antibody by invading B cells is required for the clearance of rabies virus from the central nervous system. PLoS Negl. Trop. Dis. **3:**e535. http://dx.doi.org/10.1371/journal.pntd.0000535.
78. **Fragkoudis R, Ballany CM, Boyd A, Fazakerley JK.** 2008. In Semliki Forest virus encephalitis, antibody rapidly clears infectious virus and is required to eliminate viral material from the brain, but is not required to generate lesions of demyelination. J. Gen. Virol. **89:**2565–2568. http://dx.doi.org/10.1099/vir.0.2008/002238-0.
79. **Lee H, Sunden Y, Ochiai K, Umemura T.** 2011. Experimental intracerebral vaccination protects mouse from a neurotropic virus by attracting antibody secreting cells to the CNS. Immunol. Lett. **139:**102–109. http://dx.doi.org/10.1016/j.imlet.2011.05.008.
80. **Thakare JP, Gore MM, Risbud AR, Banerjee K, Ghosh SN.** 1991. Detection of virus specific IgG subclasses in Japanese encephalitis patients. Indian J. Med. Res. **93:**271–276.
81. **Kaiser R, Dorries R, Luer W, Poser S, Pohle HD, Felgenhauer K, ter Meulen V.** 1989. Analysis of oligoclonal antibody bands against individual HIV structural proteins in the CSF of patients infected with HIV. J. Neurol. **236:**157–160. http://dx.doi.org/10.1007/BF00314332.
82. **Ryzhova E, Aye P, Harvey T, Cao W, Lackner A, Gonzalez-Scarano F.** 2009. Intrathecal humoral responses are inversely associated with the frequency of simian immunodeficiency virus macrophage-tropic variants in the central nervous system. J. Virol. **83:**8282–8288. http://dx.doi.org/10.1128/JVI.00235-09.
83. **Puccioni-Sohler M, Rios M, Bianco C, Zhu SW, Oliveira C, Novis SA, Pombo-de-Oliveira MS.** 1999. An inverse correlation of HTLV-I viral load in CSF and intrathecal synthesis of HTLV-I antibodies in TSP/HAM. Neurology **53:**1335–1339. http://dx.doi.org/10.1212/WNL.53.6.1335.
84. **Bombardieri M, Kam NW, Brentano F, Choi K, Filer A, Kyburz D, McInnes IB, Gay S, Buckley C, Pitzalis C.** 2011. A BAFF/APRIL-dependent TLR3-stimulated pathway enhances the capacity of rheumatoid synovial fibroblasts to induce AID expression and Ig class-switching in B cells. Ann. Rheum. Dis. **70:**1857–1865. http://dx.doi.org/10.1136/ard.2011.150219.
85. **Hardenberg G, Planelles L, Schwarte CM, van Bostelen L, Le Huong T, Hahne M, Medema JP.** 2007. Specific TLR ligands regulate APRIL secretion by dendritic cells in a PKR-dependent manner. Eur. J. Immunol. **37:**2900–2911. http://dx.doi.org/10.1002/eji.200737210.
86. **Xiao Y, Hendriks J, Langerak P, Jacobs H, Borst J.** 2004. CD27 is acquired by primed B cells at the centroblast stage and promotes germinal center formation. J. Immunol. **172:**7432–7441. http://dx.doi.org/10.4049/jimmunol.172.12.7432.
87. **Franciotta D, Salvetti M, Lolli F, Serafini B, Aloisi F.** 2008. B cells and multiple sclerosis. Lancet Neurol. **7:**852–858. http://dx.doi.org/10.1016/S1474-4422(08)70192-3.
88. **Owens GP, Bennett JL, Gilden DH, Burgoon MP.** 2006. The B cell response in multiple sclerosis. Neurol. Res. **28:**236–244. http://dx.doi.org/10.1179/016164106X98099.
89. **Xu W, Joo H, Clayton S, Dullaers M, Herve MC, Blankenship D, De La Morena MT, Balderas R, Picard C, Casanova JL, Pascual V, Oh S, Banchereau J.** 2012. Macrophages induce differentiation of plasma cells through CXCL10/IP-10. J. Exp. Med. **209:**1813–1823. http://dx.doi.org/10.1084/jem.20112142.
90. **Vadasz Z, Haj T, Kessel A, Toubi E.** 2013. B-regulatory cells in autoimmunity and immune mediated inflammation. FEBS Lett. **587:**2074–2078. http://dx.doi.org/10.1016/j.febslet.2013.05.023.
91. **Kalampokis I, Yoshizaki A, Tedder TF.** 2013. IL-10-producing regulatory B cells (B10 cells) in autoimmune disease. Arthritis Res. Ther. **15**(Suppl 1)**:**S1. http://dx.doi.org/10.1186/ar3907.
92. **Constant S, Schweitzer N, West J, Ranney P, Bottomly K.** 1995. B lymphocytes can be competent antigen-presenting cells for priming CD4+ T cells to protein antigens in vivo. J. Immunol. **155:**3734–3741.
93. **Lanzavecchia A, Bove S.** 1985. Specific B lymphocytes efficiently pick up, process and present antigen to T cells. Behring Inst. Mitt. **1985:**82–87.
94. **Lanzavecchia A.** 1985. Antigen-specific interaction between T and B cells. Nature **314:**537–539. http://dx.doi.org/10.1038/314537a0.
95. **van der Veen RC, Trotter JL, Kapp JA.** 1992. Immune processing of proteolipid protein by subsets of antigen-presenting spleen cells. J. Neuroimmunol. **38:**139–146. http://dx.doi.org/10.1016/0165-5728(92)90098-6.
96. **Pierson ER, Stromnes IM, Goverman JM.** 2014. B cells promote induction of experimental autoimmune encephalomyelitis by facilitating reactivation of T cells in the central nervous system. J. Immunol. **192:**929–939. http://dx.doi.org/10.4049/jimmunol.1302171.
97. **Zeng Q, Ng YH, Singh T, Jiang K, Sheriff KA, Ippolito R, Zahalka S, Li Q, Randhawa P, Hoffman RA, Ramaswami B, Lund FE, Chalasani G.** 2014. B cells mediate chronic allograft rejection independently of antibody production. J. Clin. Invest. **124:**1052–1056. http://dx.doi.org/10.1172/JCI70084.
98. **Molnarfi N, Schulze-Topphoff U, Weber MS, Patarroyo JC, Prod'homme T, Varrin-Doyer M, Shetty A, Linington C, Slavin AJ, Hidalgo J, Jenne DE, Wekerle H, Sobel RA, Bernard CC, Shlomchik MJ, Zamvil SS.** 2013. MHC class II-dependent B cell APC function is required for induction of CNS autoimmunity independent of myelin-specific antibodies. J. Exp. Med. **210:**2921–2937. http://dx.doi.org/10.1084/jem.20130699.